THE JOURNAL OF BIOLOGICAL CHEMISTRY VOL. 288, NO. 26, pp. 18975–18986, June 28, 2013

Cardiomyocyte ATP Production, Metabolic Flexibility, and Survival Require Calcium Flux through Cardiac Ryanodine Receptors *in Vivo*[*] [S]

Received for publication, October 15, 2012, and in revised form, May 14, 2013 Published, JBC Papers in Press, May 15, 2013, DOI 10.1074/jbc.M112.427062

Michael J. Bround[‡§¶‖], Rich Wambolt[**], Dan S. Luciani[‖‡‡1], Jerzy E. Kulpa[§ §§], Brian Rodrigues[¶¶], Roger W. Brownsey[§ §§], Michael F. Allard[**], and James D. Johnson[‡§¶‖2]

From the [‡]Cardiovascular Research Group, Life Sciences Institute, University of British Columbia, Vancouver V6T 1Z3, Canada, the [§]Diabetes Research Group, Life Sciences Institute, University of British Columbia, Vancouver V6T 1Z3, Canada, the [¶]Department of Cellular and Physiological Sciences, University of British Columbia, Vancouver V6T 1Z3, Canada, the [‖]Department of Surgery, University of British Columbia, Vancouver V6T 1Z3, Canada, the [**]Department of Pathology and Laboratory Medicine, University of British Columbia and the James Hogg Research Centre, St. Paul's Hospital, Vancouver V6Z 1Y6, Canada, the [‡‡]Child and Family Research Institute, Vancouver V5Z 4H4, Canada, the [§§]Department of Biochemistry and Molecular Biology, University of British Columbia, Vancouver V6T 1Z3, Canada, and the [¶¶]Department of Pharmaceutical Sciences, University of British Columbia, Vancouver BC V6T 1Z3, Canada

Background: Intracellular Ca^{2+} release has been implicated in ATP production *in vitro*.
Results: *In vivo* deletion of *Ryr2* reduces Ca^{2+}, ATP, and oxidative metabolism, leading to metabolic reprogramming and cell death.
Conclusion: RYR2 maintains cardiomyocyte ATP production and survival *in vivo*.
Significance: This work links heart metabolism to function via Ca^{2+} release from intracellular stores.

Ca^{2+} fluxes between adjacent organelles are thought to control many cellular processes, including metabolism and cell survival. *In vitro* evidence has been presented that constitutive Ca^{2+} flux from intracellular stores into mitochondria is required for basal cellular metabolism, but these observations have not been made *in vivo*. We report that controlled *in vivo* depletion of cardiac RYR2, using a conditional gene knock-out strategy (c*Ryr2*KO mice), is sufficient to reduce mitochondrial Ca^{2+} and oxidative metabolism, and to establish a pseudo-hypoxic state with increased autophagy. Dramatic metabolic reprogramming was evident at the transcriptional level via *Sirt1*/*Foxo1*/*Pgc1α*, *Atf3*, and *Klf15* gene networks. *Ryr2* loss also induced a non-apoptotic form of programmed cell death associated with increased calpain-10 but not caspase-3 activation or endoplasmic reticulum stress. Remarkably, c*Ryr2*KO mice rapidly exhibited many of the structural, metabolic, and molecular characteristics of heart failure at a time when RYR2 protein was reduced 50%, a similar degree to that which has been reported in heart failure. RYR2-mediated Ca^{2+} fluxes are therefore proximal controllers of mitochondrial Ca^{2+}, ATP levels, and a cascade of transcription factors controlling metabolism and survival.

Intracellular Ca^{2+} fluxes regulate an enormous number of processes with the specificity of responses often being ensured by spatial limitation of Ca^{2+} ions and proximity to targets. Frequently, this takes the form of Ca^{2+} signals within the nanoscale space between adjacent organelles (1). For example, *in vitro* studies have shown that Ca^{2+} flux through channels such as ryanodine receptors and IP_3 receptors mediate privileged communication between endoplasmic reticulum/sarcoplasmic reticulum (ER/SR)[3] and mitochondria and that this paces cellular metabolism by stimulating oxidative ATP production via interaction with TCA cycle enzymes (2–4). Work from Foskett and colleagues (5) recently demonstrated that knocking out IP_3 receptors in DT40 cells causes an energy-deficient state and mTor-independent autophagy. This concept has not been extended to other cell types or to the *in vivo* situation.

Ryanodine receptor Ca^{2+} channels (*e.g.* RYR2) have been observed in close proximity to mitochondria, and beat-to-beat calcium transients have been observed in cardiomyocyte mitochondria (6–8). Furthermore, we and others (9–12) have demonstrated *in vitro* that RYR2-mediated Ca^{2+} flux supports ATP levels in other cell types. In pancreatic β-cells, blocking RYR2 also induces calpain-10-dependent, caspase-3-independent, programmed cell death that is associated with presenilin-1-dependent up-regulation of hypoxia-inducible factor 1β (10, 11). To date, analysis of cellular energetics and survival in the context of reduced ER/SR Ca^{2+} channel expression has not been extended to an *in vivo* system. Ideally, the hypothesis that intracellular Ca^{2+} release is required to sustain energy metabolism *in vivo* would be tested using tissue-specific, inducible deletion of ER/SR Ca^{2+} channels.

* This work was supported by a Canadian Institutes for Health Research operating grant to J. D. J.
[S] This article contains supplemental Tables S1–S4.
[1] Supported by postdoctoral fellowships from the Canadian Diabetes Association, the Michael Smith Foundation for Health Research, and the Carlsberg Foundation.
[2] To whom correspondence should be addressed: Cardiovascular Research Group, Dept. of Cellular and Physiological Sciences & Dept. of Surgery, University of British Columbia, 5358 Life Sciences Bldg., 2350 Health Sciences Mall, Vancouver BC V6T 1Z3, Canada. Fax: 604-822-2316; E-mail: James.D.Johnson@ubc.ca.

[3] The abbreviations used are: ER/SR, endoplasmic reticulum/sarcoplasmic reticulum; IP_3, inositol 1,4,5-trisphosphate; RYR, ryanodine receptor.

The heart is an ideal model to test this hypothesis because it is a tissue with high metabolic demands. Notably, a single intracellular Ca^{2+} release channel type, RYR2, is far in excess of other analogous Ca^{2+} channels, meaning that ER/SR Ca^{2+} release may be significantly reduced with a single genetic mutation. Examination of cardiomyocytes with specific *Ryr2* gene loss-of-function is also of interest because RYR2 protein levels are known to decline as much as 50% with age, in parallel with an increased risk for heart failure (13, 14). RYR2 expression, structural organization, and function are reduced in heart failure, cardiac hypertrophy, and ischemic cardiomyopathy (15–18). It is unclear whether RYR2 loss is sufficient to cause any of the features of heart failure, including contractile dysfunction, hypertrophy, fibrosis, inflammation, transcriptional reprogramming, an energy-starved state of metabolic inflexibility, and cardiomyocyte death (19–21).

In the present study, we demonstrate that acute *in vivo* deletion of the primary ER/SR Ca^{2+} release channel reduced ATP, blunted oxidative mitochondrial metabolism, and led to inflexibility of energy substrate utilization. We provide evidence that the reduced energy state associated with loss of RYR2-mediated Ca^{2+} flux activates hypoxia-inducible factors, and switches off transcriptional control hubs that govern a range of key metabolic pathways. We further observed atypical calpain-10-dependent cell death and cardiac hypertrophy in mice following *Ryr2* knock-out. Acute *in vivo* deletion of cardiomyocyte *Ryr2* reproduces many hallmarks of heart failure, suggesting a causal, upstream role for this channel in the pathogenesis of this disease.

EXPERIMENTAL PROCEDURES

Experimental Animals—Ryr2 "floxed" mice were generated as described (22). Tamoxifen-inducible, cardiomyocyte-specific *Ryr2* knock-out mice were generated by crossing mice harboring *Ryr2* alleles containing flanking loxP sites (C57Bl6 $Ryr2^{flox/flox}$ mice) with mice expressing inducible Cre-recombinase under the control of the α-myosin heavy chain promoter (C57Bl6 mer-Cre-mer mice) (23). Tamoxifen was injected into the intraperitoneal cavity of 8–16-week-old $Ryr2^{flox/flox}$:mer-Cre-mer mice or controls for three consecutive days at 3 mg per 40 g of body weight. Protocols were approved by the University of British Columbia Animal Care Committee.

Ex Vivo Analysis of Cardiac Metabolism—Myocardial substrate utilization was measured in working hearts as detailed elsewhere (24–26). Briefly, working hearts were perfused with Krebs-Henseleit solution containing 11 mM glucose, 1.5 mM lactate, 0.15 mM pyruvate, 0.6 mM palmitate, and 20 milliunits/ml insulin. Glycolysis, as well as myocardial rates of oxidation of palmitate, glucose, and lactate were determined by the quantitative collection of ^3H_2O or $^{14}CO_2$ produced by hearts perfused with either KH solution containing [9,10-^{3}H]palmitate and [U-^{14}C]lactate or [U-^{14}C]glucose, and 5-[^{3}H]glucose.

Light and Electron Microscopy—Paraformaldehyde-fixed ventricular tissue sections were stained with H&E and Masson's trichrome to assess fibrosis. Apoptosis and cell death of adult ventricular myocytes was assessed in heart tissue sections using the TUNEL assay from Roche Applied Science according to the manufacturer's instructions. Images were taken with a Retiga-2000R camera (Q-Imaging). TUNEL-positive cells were normalized to tissue area.

Live cell imaging was conducted on cardiomyocytes isolated from c*Ryr2*KO and control mice using Langendorff reverse perfusion to introduce collagenase in to the cardiac vasculature as detailed elsewhere (27). To assess cytosolic Ca^{2+} levels, isolated cardiomyocytes were loaded with 5 μM Fura-2-AM (Invitrogen) for 30 min and washed twice for 15 min before imaging. Fura-2-AM-loaded cells were excited at 340 and 380 nm and measured for emission at 510 nm using a imaging system equipped with a 10× air objective (0.3 numerical aperture) on a Zeiss Axiovert-200 M microscope with a CoolSnapHQ2 CCD Camera (Intelligent Imaging Innovations, Denver, CO). Ratiometric images were quantified using Slidebook software (Intelligent Imaging Innovations) to measure relative cytosolic Ca^{2+} (28). To assess mitochondrial Ca^{2+} levels, isolated cardiomyocytes were loaded with 5 μM Rhod-2-AM (Invitrogen) for 30 min and washed for 15 min before imaging. In some studies, 5 μM Mitotracker Deep Red (FM) (Invitrogen) was co-loaded. Loaded cells were imaged using the Axiovert-200 M microscope described above and a 40× oil objective (1.3 numerical aperture). Rhod-2 fluorescence was used to measure relative mitochondrial Ca^{2+} (29), and Mitotracker was used to assess relative mitochondrial content for normalization. The co-loading of these dyes did not alter Ca^{2+} or cell viability (data not shown). All live-cell microscopy occurred within 8 h of isolation, and only rod-shaped cardiomyocytes with typical cell morphology were considered in analysis.

Gene, Protein, and Metabolite Analysis—Total RNA was isolated from heart tissue using TRIzol, followed by cleanup using the RNeasy kit (Qiagen). After reverse transcription (SuperScript III; Invitrogen), TaqMan quantitative RT-PCR was conducted using probes from Applied Biosystems and PerfeCTa quantitative PCR SuperMix (Quanta) on a StepOnePlus thermocycler (Applied Biosystems). SYBR Green quantitative RT-PCR was conducted using PerfeCTa SYBR Green quantitative PCR SuperMix (Quanta). Relative gene expression changes were analyzed by the $2^{-\Delta Ct}$ method and plotted in normalized relative units. Hypoxanthine-guanine phosphoribosyltransferase and cyclophilin were used as internal controls after ensuring that they were not altered in c*Ryr2*KO cardiomyocytes. Primer details are available in supplemental Tables S1–S3.

Western blot experiments were performed on lysates from mechanically disrupted hearts, homogenized, and sonicated in ice-cold lysis buffer. Samples were quantified, boiled with loading dye, and 15–50 μg of protein was used in SDS-PAGE electrophoresis. Proteins were then transferred to PVDF membranes using standard semi-dry transfer (for protein smaller than 120 kDa) or wet transfer (for proteins larger than 120 kDa) and subsequently treated with targeted primary and horseradish peroxidase-conjugated secondary antibodies. Bands were visualized using an enhanced chemiluminescence detection kit and quantified by densitometry. Antibody details can be found in supplemental Table S4. Cardiac ATP levels were assessed using standardized high-performance liquid chromatography methods (30).

Statistical Analysis—Data are expressed as mean ± S.E. unless otherwise indicated. Results were considered statistically significant when $p \leq 0.05$ using the Student's *t* test. All experiments were repeated on at least three c*Ryr2*KO mice and at least three of their tamoxifen-injected littermate controls.

RESULTS

Ryr2 Deletion Reduces Ca^{2+} Flux in Cardiac Myocytes—c*Ryr2*KO mice showed normal *Ryr2* expression until they were injected with tamoxifen, a synthetic agonist of the modified estrogen receptor:Cre fusion protein (Mer-Cre-Mer) under the control of a *αmhy6* promotor, which allowed temporally controlled targeted gene deletion of *Ryr2* in cardiomyocytes. Tamoxifen-injected littermate control mice ($Ryr2^{flox:flox}$) were used throughout the study; thus, any differences between c*Ryr2*KO and control mice cannot be attributed to tamoxifen. In our hands, this model consistently displays a >90% decrease in whole heart *Ryr2* mRNA after only 3 days of tamoxifen injections (Fig. 1*A*) (22). This leads to a time-dependent reduction in RYR2 protein levels to 51 ± 21% at 4 days post-tamoxifen and 24 ± 22% at 10 days post-tamoxifen in c*Ryr2*KO mouse hearts (22). No effects were seen in the expression of *Ryr1*, *Ryr3*, or any of the IP_3 receptor Ca^{2+} release channels (Fig. 1*A*). As expected for cells lacking their major Ca^{2+} release channel and without compensatory up-regulation of other SR channels, steady-state cytosolic Ca^{2+} was reduced in isolated, acutely cultured, non-contracting c*Ryr2*KO cardiomyocytes (Fig. 1*B*). We predicted that the loss of RYR2 channels juxtaposed with mitochondria would result in lower average Ca^{2+} levels in mitochondria. Indeed, we observed a significant decrease in steady-state mitochondrial Ca^{2+} in isolated c*Ryr2*KO cardiomyocytes (Fig. 1*C*). This result was not dependent on the normalization of the Rhod2 signal to Mitotracker fluorescence (used to control for mitochondrial number). Together, these studies suggest that loss of RYR2 in cardiomyocytes reduces Ca^{2+} flux from the SR into the mitochondria via the cytosol.

RYR2 Supports ATP Production in Vivo—In vitro studies have shown that Ca^{2+} flux from ER/SR stimulates metabolism in adjacent mitochondria (2, 3, 12). We used c*Ryr2*KO hearts to test the hypothesis that SR-to-mitochondria Ca^{2+} fluxes are required for ATP production and oxidative metabolism *in vivo*. Indeed, ATP levels were decreased in flash-frozen c*Ryr2*KO hearts (Fig. 2*A*). Consistent with this model, metabolic profiling of c*Ryr2*KO working hearts revealed significant reductions in glucose, palmitate, and lactate oxidation (Fig. 2*B*). These effects were specific to mitochondrial metabolism, as we did not observe a reduction in the rate of glycolysis (Fig. 2*C*). In fact, glycolysis was increased in c*Ryr2*KO working hearts, suggesting a compensatory mechanism and a switch toward a heart failure-like phenotype (19). These observations were made in hearts with identically oxygenated perfusate and with similar amounts of coronary artery perfusion indicating that the cardiomyocytes had similar access to metabolic substrates (Fig. 2*D*). Together, these data provide evidence that Ca^{2+} flux through RYR2 channels is essential for basal mitochondrial metabolism in the heart.

Ryr2 Deletion Leads to a Hypoxic/Ischemic State—Our previous *in vitro* work on pancreatic β-cells demonstrated that the chemical inhibitor of RyRs, ryanodine, caused a state of ATP depletion and a presenilin-1-dependent induction of hypoxia-inducible factor (11). The hypoxia-inducible factor system is a master sensor of oxidative energy use and may therefore coordinate the response to energy deprivation. Here, we also observed an increase in the levels of presenilin-1 and presenilin-2, as well as Hif1α and Hif1β (Fig. 3, *A* and *B*). A dramatic loss of uncoupling protein gene expression suggested that c*Ryr2*KO cardiomyocytes were reprogrammed to conserve and salvage energy (Fig. 3*C*). Similar to the *in vitro* observations of others (5), we observed increased autophagy, based on increased levels of LC3-II, even under conditions of nutrient availability (Fig. 3*D*). Together, these observations suggest that cardiomyocytes display complex signs of energy stress and compensation when ATP levels are reduced following RYR2 reduction.

Reprogramming of Metabolism in cRyr2KO Hearts—Given the severity of the metabolic changes, we next tested whether core transcriptional pathways had been affected by the reduction in RYR2-mediated Ca^{2+} fluxes. We focused our efforts on so-called "master regulator" pathways that modulate the expression of numerous metabolic genes in heart and other tissues. For example, we observed down-regulation of *Sirt1* and *Foxo1* (Fig. 4*A*), genes that coordinate cardiac stress responses and metabolism (31–33). Heart failure is associated with metabolic inflexibility and a switch away from fatty acid metabolism (34). Ca^{2+} signals can act via calcineurin-dependent activation of the *Ppargc1a* (Pgc1α)/*Pparα* system to sustain fatty acid oxidation (35, 36). In hearts with reduced RYR2, we observed a striking down-regulation of *Ppargc1a* and *Pparα* as well as *Pparγ* (Fig. 4*B*). Phosphoenolpyruvate carboxykinase 1 (*Pck1*), a target of Pgc1α, was virtually eliminated from c*Ryr2*KO hearts (Fig. 4*G*). The *Pparg* target gene *Cebpa* was also robustly inhibited (Fig. 4*C*). Carbohydrate responsive element-binding protein (*Chrebp*), a master regulator of complex lipid metabolism, was dramatically decreased in c*Ryr2*KO hearts (Fig. 4*C*). Accordingly, expression of ATP-citrate lyase (*Acly*) and acetyl-CoA carboxylase β (*Acacb*) were decreased significantly; expression of stearoyl-coenzyme A desaturase 1 (*Scd1*) was virtually eliminated (Fig. 4, *D* and *E*). The reduction in lipogenic enzymes was associated with down-regulation of fat transporters (Fig. 4*F*). At the same time, we observed a dramatic decrease in expression of genes encoding hormone sensitive lipase (*Hsl*), adiponutrin (*Adpn*), and adipose triglyceride lipase (*Atgl*) (Fig. 4*H*). *Atgl* is essential for degrading lipid droplets and mice lacking this gene have fatty, hypertrophied, and failing hearts (37). Interesting, we noted reduced expression of the genes encoding the GLUT4 glucose transporter and phosphoenolpyruvate carboxykinase 1 (Fig. 4, *G* and *I*). Together, these data suggest that the use of lipids and other substrates by the c*Ryr2*KO heart may be abrogated and provide novel insight into the link between Ca^{2+} and metabolism.

Ryr2 Deletion Induces Programmed Cell Death—Heart failure is associated with an increase in cardiomyocyte death, which can be apoptotic, non-apoptotic, and/or associated with ER stress depending on the model (21). c*Ryr2*KO hearts contained numerous TUNEL-positive cells, which were virtually absent in controls (Fig. 5, *A* and *B*). This cell death was not

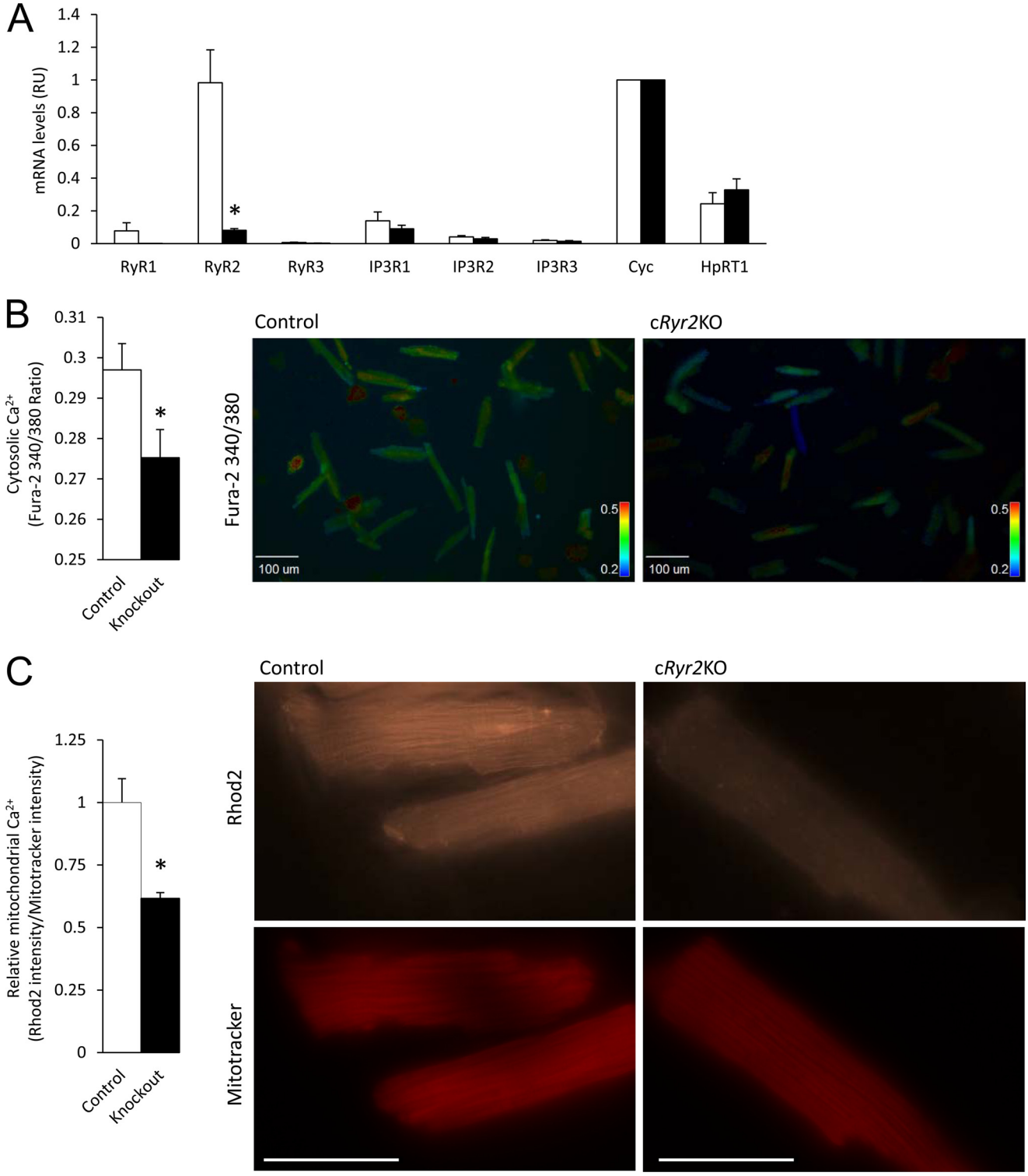

FIGURE 1. **Acute cardiac-specific *Ryr2* gene ablation without compensation from related Ca^{2+} channels.** *A*, SR/ER Ca^{2+} release channel mRNA levels in heart tissue 10 days after tamoxifen injection. Data are normalized to cyclophilin D (*Cyc*) levels ($n = 6$). *White bars*, control mice; *Black bars*, c*Ryr2*KO mice. *B*, reduced basal cytosolic Ca^{2+} levels in isolated, acutely cultured, unstimulated cardiomyocytes from c*Ryr2*KO mice. Data are from at least three independent cell preparations (control cells $n = 124$; c*Ryr2*KO cells $n = 210$). *C*, reduced basal mitochondrial luminal Ca^{2+} levels in isolated, unstimulated cardiomyocytes from c*Ryr2*KO mice. Data are from four independent cell preparations (control cells ($n = 170$); c*Ryr2*KO cells ($n = 180$); *, $p \leq 0.05$). *White scale bars* indicate 20 μm. *, $p \leq 0.05$. *RU*, relative units; IP3R, IP_3 receptor.

caused by ER stress because we observed a decrease in CHOP expression and other ER stress markers (Fig. 5, *C* and *D*). In some cell types, RYR2 hyperactivity contributes to classical caspase-3-dependent apoptosis (28). However, we discovered previously that inhibiting RYR2-mediated Ca^{2+} flux with ryanodine caused caspase-3-independent programmed cell death (10). c*Ryr2*KO hearts did not exhibit a significant increase in caspase-3 cleavage (Fig. 5*E*), confirming our hypothesis that

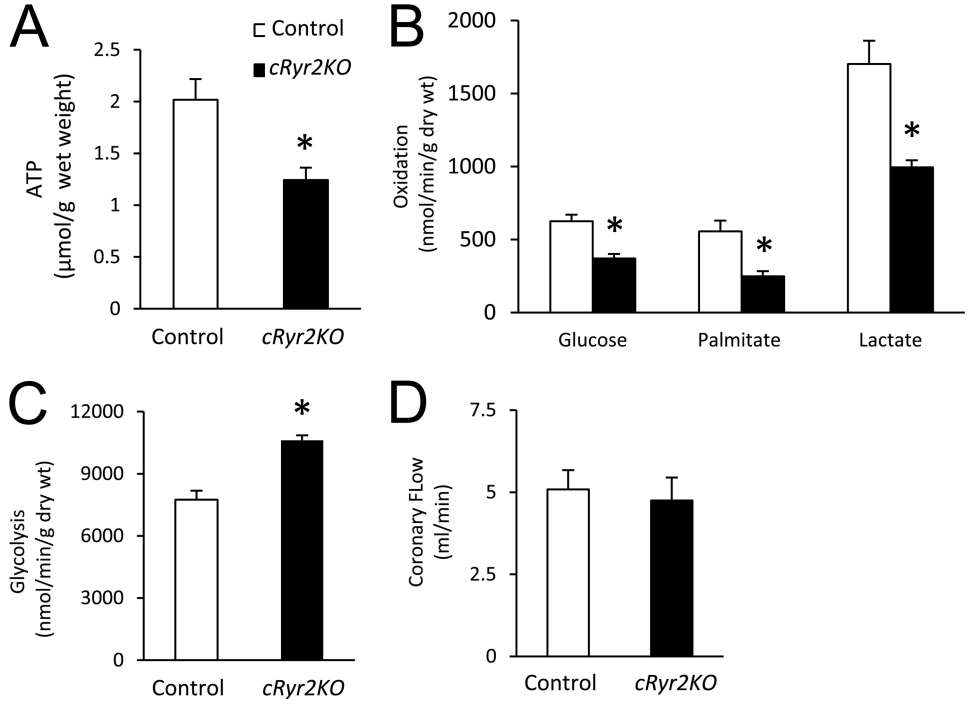

FIGURE 2. **Loss of RYR2-mediated Ca^{2+} flux reduces mitochondrial metabolism and steady-state ATP levels.** *A*, ATP levels of freshly excised and freeze clamped hearts ($n = 9$). *White bars*, control; *black bars*, c*Ryr2*KO. *B*, oxidation rates of glucose, palmitate, and lactate by isolated, perfused working hearts (control, $n = 3$; c*Ryr2*KO, $n = 4$). *C*, rates of glycolysis during working heart preparation (control, $n = 3$; c*Ryr2*KO, $n = 4$). *D*, coronary arterial flow during the working heart perfusions when metabolic assessments were made (control, $n = 6$; c*Ryr2*KO, $n = 8$). All data were collected 4 days after the first tamoxifen injection. *, $p \leq 0.05$.

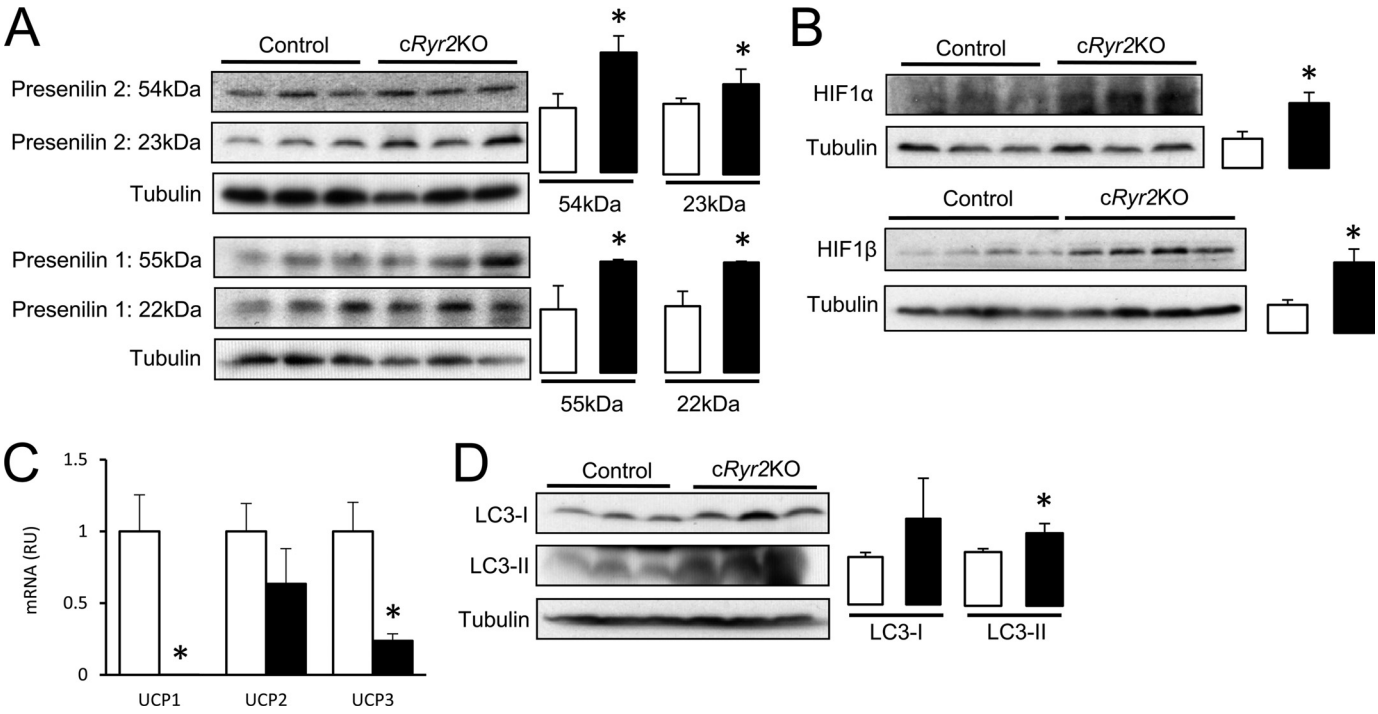

FIGURE 3. **Acute *Ryr2* ablation causes a hypoxia-like cellular state.** *A*, presenilin-1 (22 and 55 kDa) and presenilin-2 (23 and 54 kDa) protein levels. *White bars*, control; *black bars*, c*Ryr2*KO throughout. Individual blot lanes are biological replicates throughout ($n = 3$). *B*, Hif1α (120 kDa) and Hif1β (95 kDa) protein levels (HIF1α, $n = 3$; HIF1β, $n = 7$). *C*, uncoupling protein mRNA ($n = 3$). *D*, autophagy marker LC3-I (18 kDa) and LC3-II (16 kDa) ($n = 3$). Protein quantification plots represent relative expression normalized to tubulin (50 kDa). All data were collected 4 days after the first tamoxifen injection. *, $p \leq 0.05$. *RU*, relative units.

RYR2 suppresses an atypical form of non-apoptotic cell death. We observed a reduction in the expression of the prosurvival gene *Bcl2*, perhaps further contributing to cell death (Fig. 5*F*). We have previously shown that calpain-10 mRNA and small molecular weight isoforms of calpain-10 are up-regulated in cells with depressed energy state resulting from ryanodine

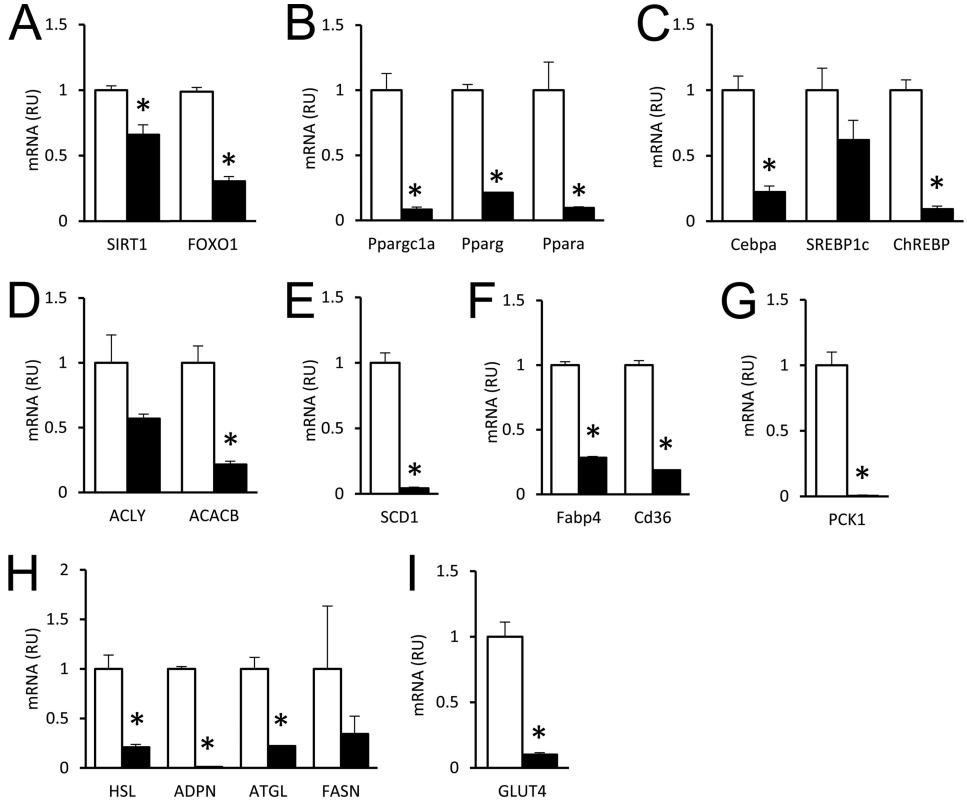

FIGURE 4. **Conditional *Ryr2* knock-out results in metabolic reprogramming at the transcriptional level.** *A–I*, expression of key metabolic gene mRNA in whole heart was measured 4 days post-tamoxifen using Taqman RT-quantitative PCR. We measured mRNA expression levels of sirtuin 1 (*SIRT1*; *A*), forkhead box O1 (*FOXO1*; *A*), peroxisome proliferator-activated receptor γ, coactivator 1 α (*Ppargc1a*; *B*), peroxisome proliferator-activated receptor γ (*Pparg*; *B*), peroxisome proliferator-activated receptor α (*Ppara*; *B*), CCAAT/enhancer binding protein (*C/EBP*) α (*Cebpa*; *C*), sterol regulatory element binding transcription factor 1 (*SREBP1c*; *C*), carbohydrate response element-binding protein (*ChREBP*; *C*), ATP citrate lyase (*ACLY*; *D*), acetyl-CoA carboxylase β (*ACACB*; *D*), stearoyl-coenzyme A desaturase 1 (*SCD1*; *E*), fatty acid binding protein 4, adipocyte (*Fabp4*; *F*), CD36 molecule (*CD36*; *F*), phosphoenolpyruvate carboxykinase 1, cytosolic (*Pck1*; *G*), hormone-sensitive lipase (*HSL*; *H*), adiponutrin (*ADPN*; *H*), adipose triglyceride lipase (*ATGL*; *H*), fatty acid synthase (*FASN*; *H*), and solute carrier family 2 (facilitated glucose transporter), member 4 (*GLUT4*; *I*). *White bars*, control; *black bars*, c*Ryr2*KO throughout ($n = 3$). All data were collected 4 days after the first tamoxifen injection. *, $p \leq 0.05$. *RU*, relative units.

treatment (10, 11). Two protein isoforms of calpain-10 were significantly increased in heart tissue from c*Ryr2*KO mice (Fig. 5*G*). These bands likely represent calpain-10 protein isoforms and cleavage products, as they are not observed in tissue from calpain-10 knock-out mice (10). No effects were observed on the levels of calpain-1 or calpain-2 protein in c*Ryr2*KO hearts. Thus, loss of Ryr2 function activates a conserved form of calpain-10-associated programmed cell death in multiple tissues, including the heart.

Loss of Cardioprotective Pathways in cRyr2KO Hearts—Cell death can be accelerated when growth factor signaling pathways are down-regulated, and hypoxia-like conditions have been linked to insulin resistance (38). c*Ryr2*KO hearts had a significant reduction in the mRNA and protein levels of the insulin receptor (Fig. 5, *H* and *K*). A trend toward increased *Ptpn1* expression further suggested a suppression of insulin signaling (Fig. 5*H*), and this was supported by a significant reduction in ERK activity and prosurvival AKT phosphorylation at threonine 308 (Fig. 5*K*). Cardioprotective adiponectin and leptin signaling systems were down-regulated (Fig. 5, *I* and *J*). These data suggest that survival pathways are reduced following *Ryr2* reduction.

Ryr2 Deletion Causes Cardiac Hypertrophy and Fibrosis—c*Ryr2*KO mice represented an ideal tool to test the hypothesis that acute cardiomyocyte stress and dysfunction is sufficient to induce cardiac hypertrophy. We observed an increase in gross heart volume and mass (Fig. 6*A*), and heart fibrosis in c*Ryr2*KO mice (Fig. 6*B*), already evident 10 days after tamoxifen injection. Many chronic models of cardiac hypertrophy result in a re-expression of fetal genes, including cardioprotective growth factors. In our acute model, brain natriuretic peptide transcription was significantly increased, and adult β-myosin heavy chain gene (*Mhy6*) was attenuated (Fig. 6, *C* and *D*), but we did not find a simultaneous up-regulation of the fetal β-myosin heavy chain gene (*Mhy7*; Fig. 6*D*). Interestingly, we observed a reduction of cleaved *Notch1* (Fig. 6*E*), which plays a key role in maintaining cardiac progenitors (39). Heart failure can be associated with an increase in cardiac inflammation and the local release of proinflammatory cytokines (40). We observed a dramatic 20-fold increase in interleukin-6 transcription in c*Ryr2*KO hearts (Fig. 6*F*). *Ryr2* may therefore be upstream of some, but not all, aspects of cardiac inflammation.

Next, we examined pathways that could translate the effects of stress into a hypertrophic pathology. *Atf3*, a stress gene activated by ischemia/hypoxia (41, 42), was increased ~2.5-fold in c*Ryr2*KO hearts (Fig. 6*G*). Cardiac *Atf3* overexpression is sufficient to induce cardiomyopathy, hypertrophy, and myocyte death (43). We also observed a dramatic loss of several genes

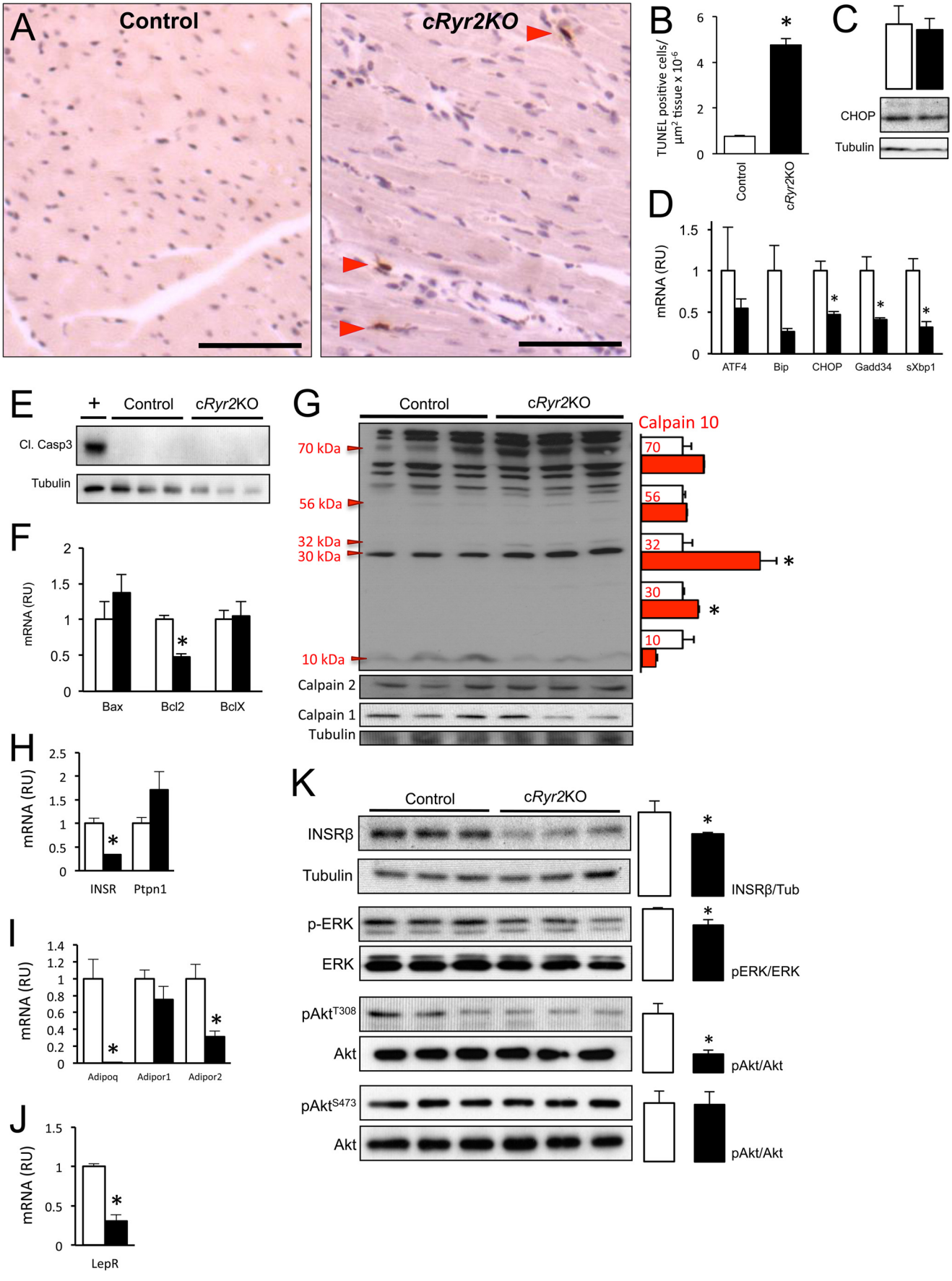
A
Control
cRyr2KO
B
TUNEL positive cells/ µm² tissue x 10⁻⁶
Control
cRyr2KO
C
CHOP
Tubulin
D
mRNA (RU)
ATF4
Bip
CHOP
Gadd34
sXbp1
E
+
Control
cRyr2KO
Cl. Casp3
Tubulin
F
mRNA (RU)
Bax
Bcl2
BclX
G
Control
cRyr2KO
Calpain 10
70 kDa
56 kDa
32 kDa
30 kDa
10 kDa
Calpain 2
Calpain 1
Tubulin
H
mRNA (RU)
INSR
Ptpn1
I
mRNA (RU)
Adipoq
Adipor1
Adipor2
J
mRNA (RU)
LepR
K
Control
cRyr2KO
INSRβ
Tubulin
INSRβ/Tub
p-ERK
ERK
pERK/ERK
pAktT308
Akt
pAkt/Akt
pAktS473
Akt
pAkt/Akt

negatively regulated by *Atf3*, including *Glut4* (Fig. 4*I*). c*Ryr2*KO also resulted in a near complete loss of *Klf15* (Fig. 6*H*), which, based on knock-out studies, is sufficient to induce heart failure and fibrosis (44, 45). *Klf15* is a positive regulator of *Ucp1* and *Pparg* (46), genes that were decreased in c*Ryr2*KO hearts. Thus, acute *Ryr2* knock-out and the concomitant energy-deficient state have profound effects on transcriptional hubs, controlled, at least in part, by hypoxia-inducible factors, *Klf15*, *Atf3*, and *Foxo1*/*Sirt1*.

Throughout this study, we assessed the survival of c*Ryr2*KO mice. Despite molecular and/or physical compensation, c*Ryr2*KO mice invariably met their humane end point after a period that could range from days to weeks, as we have shown previously (22). Thus, the cardiac expression of the *Ryr2* gene is essential for survival in adult mice.

DISCUSSION

The purpose of this study was to test the hypothesis that Ca^{2+} flux from intracellular stores, in this case through cardiomyocyte SR RYR2 channels, is required to maintain cellular energy homeostasis and survival *in vivo*. We used tissue-specific inducible gene ablation to examine the *in vivo* functions of *Ryr2* in the adult mouse heart. This model circumvents the embryonic lethality of $Ryr2^{-/-}$ mice (47), as well as the possible long term compensation from related Ca^{2+} channels reported in $Ryr2^{+/-}$ mice (48). Our *in vivo* mouse studies support the concept, previously proposed after *in vitro* studies (5), that intracellular Ca^{2+} release paces mitochondrial metabolism and protects cells from atypical programmed cell death caused by energy depletion (Fig. 6*I*). Our data extend this concept to include the Ca^{2+}-dependent control of key transcription factor networks that modulate metabolic substrate utilization. Our results also demonstrate that partial loss of cardiomyocyte RYR2 protein is sufficient to recapitulate many of the characteristics of human heart failure, providing new mechanistic insight into this devastating condition.

In the physiological state, the cardiomyocyte is always working. Our analysis of metabolism and survival were conducted *in vivo* and in *ex vivo* working heart models. The single-cell Ca^{2+} measurements were the only experiments in this study not conducted in working cardiomyocytes. Nevertheless, these measurements provide some interesting information and suggest a role for RYR2 channels in cardiomyocyte Ca^{2+} homeostasis. Taken at face value, these data suggest that basal Ca^{2+} flux through RYR2 channels normally supports a significant component of resting Ca^{2+} levels in both the cytosolic and mitochondrial compartments of isolated cardiomyocytes. Indeed, microscopic and submicroscopy RYR2-mediated Ca^{2+} release events have previously been implicated in the diastolic SR Ca^{2+} leak into the cytosol (49), and subthreshold RYR2 release events are known to increase Ca^{2+} in nearby mitochondria (50). Future studies will be required to assess Ca^{2+} in these compartments in beating cardiomyocytes, ideally within the intact heart.

One of the key findings of our study is that c*Ryr2*KO mouse hearts had decreased ATP levels, as well as lower substrate utilization when compared with control hearts. This can be attributed to defects in the utilization of metabolic substrates via oxidative ATP generation. The Ca^{2+} dependence of the TCA cycle was proposed many years ago based on the finding that Ca^{2+} in the matrix of isolated mitochondria stimulates several enzymes in the pathway, including pyruvate dehydrogenase, which controls entry of glucose carbon into the TCA cycle (4, 51, 52). Similarly, emerging evidence suggests that the F_1F_0 ATP synthase is also directly regulated by mitochondrial Ca^{2+} such that the maximal rate of oxidative ATP production at given mitochondrial membrane potential is dependent on Ca^{2+} concentration (12). As such, the rate and efficacy of many energy-producing substrates via the TCA cycle could be affected by mitochondrial Ca^{2+} dynamics. Collectively, these enzymes are thought to rely on Ca^{2+} signals from across nanoscale spaces between ER/SR and mitochondria. Local microdomains of concentrated Ca^{2+} are required to access the mitochondria and the duration of the mitochondrial Ca^{2+} transients is limited by rapid export mechanisms (2, 3, 6). Our results suggest that ablation of RYR2 *in vivo* disrupts this signaling pathway, leading to a decrease in TCA cycle enzymatic activity and, consequently, a diminished ability to sustain cellular ATP levels. Inability to employ the TCA cycle likely promotes the metabolic inflexibility observed in heart failure, as the utilization of fat as fuel requires oxidative metabolism (19). Indeed, decreased RYR2 expression or function is associated with several models of metabolic cardiomyopathy (15–18). Our data support the concept that decreased RYR2 function in cardiac pathology may directly contribute to metabolic inflexibility seen in heart failure.

Our data also provide evidence for a role for RYR2 and Ca^{2+} in regulating lipid utilization and ATP production by transcriptional reprogramming. It is well established that failing hearts switch from metabolizing free fatty acids toward carbohydrate utilization (19). Knock-out and overexpression studies show that changes in transcriptional regulators and enzymes involved in lipid metabolism are sufficient to cause cardiac hypertrophy and steatosis (35, 37, 53). Our data suggest a role of the cytoprotective and metabolism-controlling *Sirt1*/*Foxo1*/*Pgc1α* axis in hearts lacking *Ryr2*. RYR2 deficiency is sufficient to flip a transcriptional metabolic "master switch," which down-regulates lipid utilization pathways and effectors. We

FIGURE 5. **Acute *Ryr2* ablation causes calpain-10 dependent programmed cell death.** *A*, representative imagines of TUNEL staining (*arrows*) of fixed heart sections (*scale bar*, 100 μm). *B*, quantification of TUNEL-positive nuclei (control, $n = 4$; c*Ryr2*KO, $n = 5$). *White bars*, control; *black bars*, c*Ryr2*KO throughout. *C*, ER stress gene expression ($n = 3$). *D*, CHOP (31 kDa) protein expression ($n = 7$). *E*, cleaved caspase-3 (*Cl. Casp3*; 19 kDa) protein levels. +, a positive cleaved caspase-3 control sample (thapsigargin-treated MIN6 cells). Individual blot lanes are biological replicates throughout ($n = 3$). *F*, cell death effecter gene expression 4 days post tamoxifen injection ($n = 3$). *G*, calpain-10 protein levels and expression patterns. Calpain-1 (80 kDa) and calpain-2 (80 kDa) levels are also displayed. *White bars*, control; *red bars*, c*Ryr2*KO. *H*, insulin receptor (*INSR*) and *Ptpn1* gene expression levels ($n = 3$). *I*, adiponectin and adiponectin receptor (*Adipor*) mRNA expression ($n = 3$). *J*, leptin receptor (*LepR*) mRNA ($n = 3$). *K*, expression and/or phosphorylation states of insulin receptor (*INSR*; 190 and 95 kDa), Akt (60 kDa), and Erk (42 and 44 kDa) ($n = 3$). All analyses carried out 4 days post-tamoxifen treatment. Protein quantification plots represent relative expression normalized to either total protein or to tubulin (*Tub*; 50 kDa). TUNEL data were collected 10 days following tamoxifen treatment; all other data collected 4 days following the first tamoxifen injection. *, $p \leq 0.05$. *S473*, Ser-473; *T308*, Thr-308.

also found reduced insulin signaling and dramatic loss of *Glut4*, which might be expected to have deleterious effects given the cardioprotective effect of glucose uptake (54). Therefore, our study suggests that acute *Ryr2* deletion disrupts both lipid and carbohydrate metabolism indirectly via transcriptional programming, as well as directly at the mitochondria.

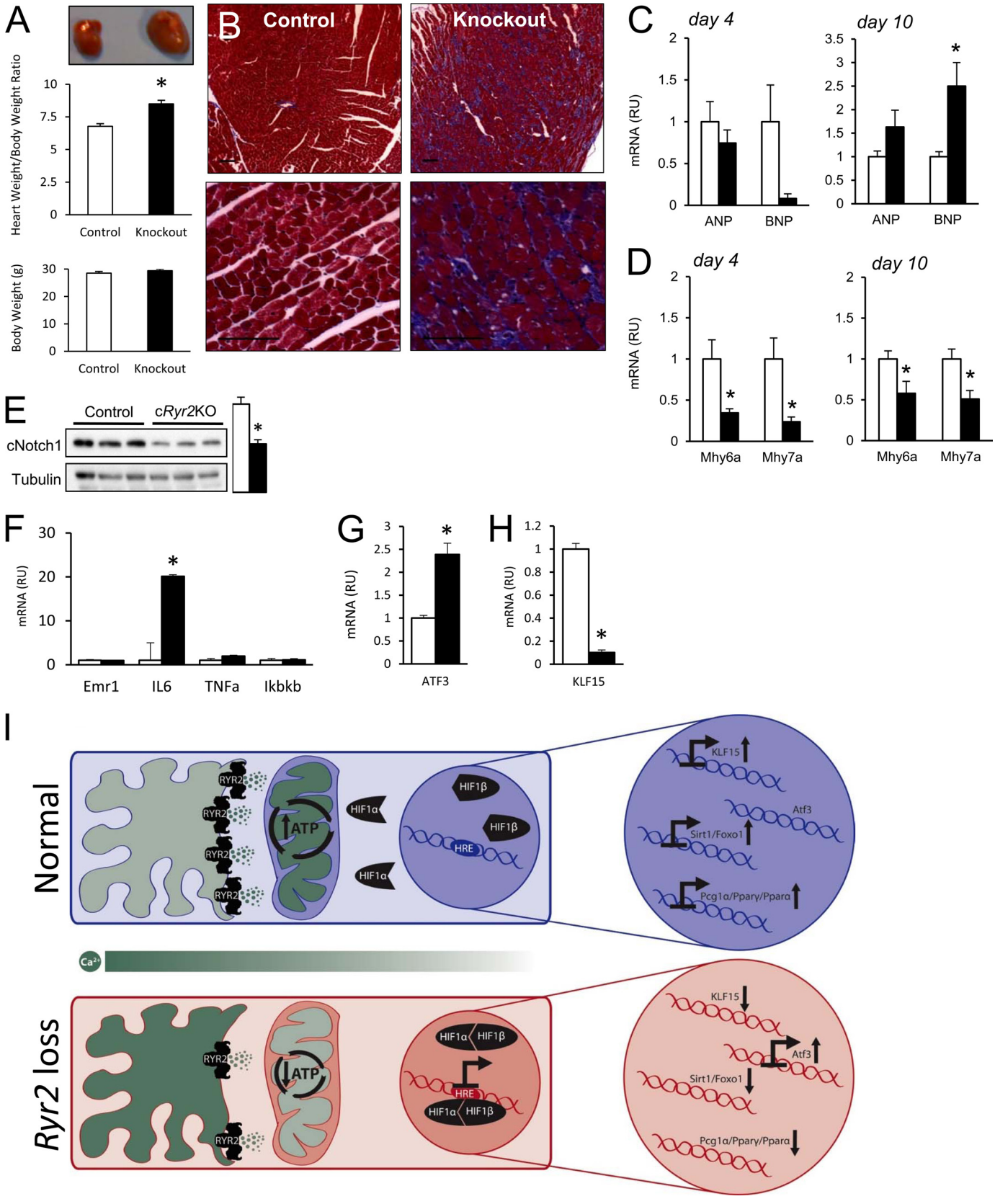

In our previous studies of other cell types, loss of metabolism-pacing Ca^{2+} communication between RyR channels and mitochondria caused cellular ATP levels to decline and induced the presenilin-dependent expression of key hypoxia response genes (3, 11). Similarly, c*Ryr2*KO mice had significantly increased proteins levels of presenilin-1, presenilin-2, HIF1α, and HIF1β, and they displayed numerous signs of energy starvation with an associated increase in compensatory mechanisms for energy conservation and optimization. This included decreased expression of uncoupling proteins and down-regulated carbohydrate and lipid storage pathways. Thus, c*Ryr2*KO hearts exist in a pseudohypoxic stress state. Hypoxia-inducible factors are known to increase *Atf3* and decrease *Klf15* expression, a combination of events that is sufficient to drive cardiomyopathy, hypertrophy, fibrosis, and cell death (41, 43, 45, 55). Although we cannot rule out other parallel mechanisms of cardiac dysfunction in other models of heart failure, our evidence does demonstrate that disruption of RYR2-dependent metabolism is sufficient to cause heart failure.

Pharmacological studies have shown that Ca^{2+} released through RYRs or IP_3 receptors into adjacent mitochondria modulates apoptosis (9, 50). When in excess, Ca^{2+} transfer from SR/ER to mitochondria triggers caspase-3-dependent apoptosis (28). We and others (9, 10, 56) have shown that constitutive intracellular Ca^{2+} signals are required to stimulate cellular respiration and prevent a hypoxia-like state with calpain-dependent, caspase-3-independent cell death. Interestingly, calpain-10 is localized to mitochondria (57) where it is poised to sense metabolic state. Our data indicate that disruption of RYR2 function, via its effects on mitochondrial calcium signaling and cellular metabolism, is also sufficient to cause cell death *in vivo*. Additional work will be required to further elucidate the mechanisms involved in this atypical cell death mode. We found evidence of autophagy in c*Ryr2*KO hearts similar to the data on cells lacking IP_3 receptors (5), suggesting that the control of metabolism and autophagy by SR/ER-to-mitochondria Ca^{2+} shuttling, both the barely perceptible Ca^{2+} microsignaling from stochastic channel opening as well as the larger global Ca^{2+} signals found in excitable cells such as cardiomyocytes, may be a ubiquitous metabolic control system.

Our inducible knock-out approach was designed to mitigate chronic compensatory gene expression induced by lifelong genetic alterations. Accordingly, our data were not confounded by compensation from other ER/SR Ca^{2+} release channels. We speculate that this may be the reason for the discrepancy between our observations of cardiac hypertrophy and the results obtained in mice with chronic *Ryr2* haploinsufficiency, which were protected from pressure overload-induced hypertrophy (48). Interestingly, increased levels of cell death were reported in $Ryr2^{+/-}$ mice. The majority of *in vivo* studies of *Ryr2* have used point mutation knock-in mice, typically with gain-of-function mutations causing "leaky channels" (58, 59). Studies have focused on the susceptibility of these mice to tachycardic arrhythmia. Recently, a loss-of-function knock-in model was created ($Ryr2^{ADA/ADA}$ mice) and reported to undergo calcineurin-independent hypertrophy (60). Additional studies are required to determine whether the hypertrophy observed in our c*Ryr2*KO hearts is mediated through a similar mechanism. Given the fact that basal cytosolic Ca^{2+} appears to be lower in c*Ryr2*KO cardiomyocytes, one might speculate that a calcineurin-independent pathway is involved.

Although ours is the first *in vivo* study to target an intracellular Ca^{2+} channel and examine metabolism, our conclusions are well supported by more reductionist studies on the roles of RYR2 in cardiac metabolism (2–5, 12), cell survival (10, 11, 48), and cardiac dysfunction (15–17). In our model, deletion of *Ryr2* rapidly led to many alterations in cardiac phenotype. Because our only manipulation was *Ryr2* deletion, all of the observed changes must ultimately be downstream of RYR2 action in cardiomyocytes, either immediately downstream or indirectly downstream. Future studies are required to elucidate the specific mechanisms involved and the temporal order in which these events occur.

In summary, our results illustrate that Ca^{2+} flux through the ER/SR RYR2 Ca^{2+} channels is required to maintain mitochondrial Ca^{2+}, oxidative metabolism, metabolic transcriptional pathways, and cellular survival in the mouse heart *in vivo*. These observations, which support concepts advanced from *in vitro* studies, demonstrate a paramount role for RYR2 in cardiomyocyte energetics. This creates a paradigm in which RYR2 Ca^{2+} fluxes have simultaneous roles in the regulation of heart rate and rhythmicity (22), as well as effects on metabolic mitochondrial pacing, and transcriptional programming in cardiomyocytes. This comprehensive model may explain how functional and metabolic demands of cardiomyocytes can be so exquisitely coupled to ensure energy needs are met.

Acknowledgments—We thank Edwin Moore for helpful comments throughout this project. We thank Dr. Tatyana B. Kalynyak, Xiaoke Hu, Farnaz Taghizadeh, and Saba Marzara for technical assistance. We thank Kenneth Boheler (University of Hong Kong) for helpful comments throughout this project and for providing the original line of $Ryr2^{flox/flox}$ *mice.*

FIGURE 6. **Cardiac hypertrophy and fibrosis in *cRyr2KO* hearts.** *A*, heart size, heart wet weight relative to body mass, and total body mass 10 days following tamoxifen treatment (control, $n = 6$; c*Ryr2*KO, $n = 8$; *, $p \leq 0.05$). The image is representative. *B*, Masson's trichrome staining of cardiac tissue sections collected 10 days following tamoxifen treatment. *Lower panels* are higher magnification images of *top panels*. Images are representative (control, $n = 4$; c*Ryr2*KO, $n = 5$; *scale bar*, 100 μm). *C* and *D*, *Anp*, *Bnp*, *Mhy6*, and *Mhy7* gene expression 4 and 10 days after tamoxifen treatment ($n = 3$). *E*, cleaved Notch1 (110 kDa) protein at 4-days post-tamoxifen. Individual blot lanes are biological replicates throughout ($n = 3$). *F*, inflammatory gene expression 4 days post-tamoxifen ($n = 3$). *G* and *H*, gene expression levels of ATF3 and KLF15 assessed 4 days post-tamoxifen ($n = 3$). Protein quantification plots represent relative expression normalized to either total protein or to tubulin (50 kDa). *I*, a schematic summarizing the observed effects of *Ryr2* deletion on cardiomyocyte energy metabolism. The *top panel* depicts a normal situation where calcium from the SR/ER enters the mitochondria via RYR2, where it stimulates oxidative metabolism and maintains a normal cardiac transcriptional program. The *bottom panel* depicts a situation where there is reduced RYR2 signaling resulting in less calcium entering the mitochondria, which blunts oxidative ATP metabolism. This activates hypoxia-inducible transcription factors, which, along with alternate pathways, alters the cardiac transcriptional programming in a manner associated with cardiac pathology. *, $p \leq 0.05$. *HRE,* hypoxia-response element.

REFERENCES

1. Johnson, J. D., Bround, M. J., White, S. A., and Luciani, D. S. (2012) Nanospaces between endoplasmic reticulum and mitochondria as control centres of pancreatic β-cell metabolism and survival. *Protoplasma* **249,** S49–58
2. Giacomello, M., Drago, I., Bortolozzi, M., Scorzeto, M., Gianelle, A., Pizzo, P., and Pozzan, T. (2010) Ca^{2+} hot spots on the mitochondrial surface are generated by Ca^{2+} mobilization from stores, but not by activation of store-operated Ca^{2+} channels. *Mol. Cell* **38,** 280–290
3. Liu, T., and O'Rourke, B. (2008) Enhancing mitochondrial Ca^{2+} uptake in myocytes from failing hearts restores energy supply and demand matching. *Circ. Res.* **103,** 279–288
4. Denton, R. M., and McCormack, J. G. (1990) Ca^{2+} as a second messenger within mitochondria of the heart and other tissues. *Annu. Rev. Physiol.* **52,** 451–466
5. Cárdenas, C., Miller, R. A., Smith, I., Bui, T., Molgó, J., Müller, M., Vais, H., Cheung, K. H., Yang, J., Parker, I., Thompson, C. B., Birnbaum, M. J., Hallows, K. R., and Foskett, J. K. (2010) Essential regulation of cell bioenergetics by constitutive InsP3 receptor Ca^{2+} transfer to mitochondria. *Cell* **142,** 270–283
6. Kettlewell, S., Cabrero, P., Nicklin, S. A., Dow, J. A., Davies, S., and Smith, G. L. (2009) Changes of intra-mitochondrial Ca2+ in adult ventricular cardiomyocytes examined using a novel fluorescent Ca^{2+} indicator targeted to mitochondria. *J. Mol. Cell Cardiol.* **46,** 891–901
7. Salnikov, V., Lukyanenko, Y. O., Lederer, W. J., and Lukyanenko, V. (2009) Distribution of ryanodine receptors in rat ventricular myocytes. *J. Muscle Res. Cell Motil.* **30,** 161–170
8. Lukyanenko, V., Ziman, A., Lukyanenko, A., Salnikov, V., and Lederer, W. J. (2007) Functional groups of ryanodine receptors in rat ventricular cells. *J. Physiol.* **583,** 251–269
9. Tsuboi, T., da Silva Xavier, G., Holz, G. G., Jouaville, L. S., Thomas, A. P., and Rutter, G. A. (2003) Glucagon-like peptide-1 mobilizes intracellular Ca^{2+} and stimulates mitochondrial ATP synthesis in pancreatic MIN6 β-cells. *Biochem. J.* **369,** 287–299
10. Johnson, J. D., Han, Z., Otani, K., Ye, H., Zhang, Y., Wu, H., Horikawa, Y., Misler, S., Bell, G. I., and Polonsky, K. S. (2004) RyR2 and calpain-10 delineate a novel apoptosis pathway in pancreatic islets. *J. Biol. Chem.* **279,** 24794–24802
11. Dror, V., Kalynyak, T. B., Bychkivska, Y., Frey, M. H., Tee, M., Jeffrey, K. D., Nguyen, V., Luciani, D. S., and Johnson, J. D. (2008) Glucose and endoplasmic reticulum calcium channels regulate HIF-1β via presenilin in pancreatic β-cells. *J. Biol. Chem.* **283,** 9909–9916
12. Glancy, B., and Balaban, R. S. (2012) Role of mitochondrial Ca^{2+} in the regulation of cellular energetics. *Biochemistry* **51,** 2959–2973
13. Kandilci, H. B., Tuncay, E., Zeydanli, E. N., Sozmen, N. N., and Turan, B. (2011) Age-related regulation of excitation-contraction coupling in rat heart. *J. Physiol. Biochem.* **67,** 317–330
14. Assayag, P., CHarlemagne, D., Marty, I., de Leiris, J., Lompré, A. M., Boucher, F., Valére, P. E., Lortet, S., Swynghedauw, B., and Besse, S. (1998) Effects of sustained low-flow ischemia on myocardial function and calcium-regulating proteins in adult and senescent rat hearts. *Cardiovasc. Res.* **38,** 169–180
15. Bidasee, K. R., Dinçer, U. D., and Besch, H. R., Jr. (2001) Ryanodine receptor dysfunction in hearts of streptozotocin-induced diabetic rats. *Mol. Pharmacol.* **60,** 1356–1364
16. Naudin, V., Oliviero, P., Rannou, F., Sainte Beuve, C., and Charlemagne, D. (1991) The density of ryanodine receptors decreases with pressure overload-induced rat cardiac hypertrophy. *FEBS Lett.* **285,** 135–138
17. Brillantes, A. M., Allen, P., Takahashi, T., Izumo, S., and Marks, A. R. (1992) Differences in cardiac calcium release channel (ryanodine receptor) expression in myocardium from patients with end-stage heart failure caused by ischemic versus dilated cardiomyopathy. *Circ. Res.* **71,** 18–26
18. Matsui, H., MacLennan, D. H., Alpert, N. R., and Periasamy, M. (1995) Sarcoplasmic reticulum gene expression in pressure overload-induced cardiac hypertrophy in rabbit. *Am. J. Physiol.* **268,** C252–258
19. Stanley, W. C., Recchia, F. A., and Lopaschuk, G. D. (2005) Myocardial substrate metabolism in the normal and failing heart. *Physiol. Rev.* **85,** 1093–1129
20. Crossman, D. J., Ruygrok, P. N., Ruygrok, P. R., Soeller, C., and Cannell, M. B. (2011) Changes in the organization of excitation-contraction coupling structures in failing human heart. *PLoS One* **6,** e17901
21. Ferrari, R., Ceconi, C., Campo, G., Cangiano, E., Cavazza, C., Secchiero, P., and Tavazzi, L. (2009) Mechanisms of remodelling: a question of life (stem cell production) and death (myocyte apoptosis). *Circ. J.* **73,** 1973–1982
22. Bround, M. J., Asghari, P., Wambolt, R. B., Bohunek, L., Smits, C., Philit, M., Kieffer, T. J., Lakatta, E. G., Boheler, K. R., Moore, E. D., Allard, M. F., and Johnson, J. D. (2012) Cardiac ryanodine receptors control heart rate and rhythmicity in adult mice. *Cardiovasc. Res.* **96,** 372–380
23. Sohal, D. S., Nghiem, M., Crackower, M. A., Witt, S. A., Kimball, T. R., Tymitz, K. M., Penninger, J. M., and Molkentin, J. D. (2001) Temporally regulated and tissue-specific gene manipulations in the adult and embryonic heart using a tamoxifen-inducible Cre protein. *Circ. Res.* **89,** 20–25
24. Allard, M. F., Schönekess, B. O., Henning, S. L., English, D. R., and Lopaschuk, G. D. (1994) Contribution of oxidative metabolism and glycolysis to ATP production in hypertrophied hearts. *Am. J. Physiol.* **267,** H742–H750
25. Belke, D. D., Larsen, T. S., Lopaschuk, G. D., and Severson, D. L. (1999) Glucose and fatty acid metabolism in the isolated working mouse heart. *Am. J. Physiol.* **277,** R1210–1217
26. Khairallah, M., Labarthe, F., Bouchard, B., Danialou, G., Petrof, B. J., and Des Rosiers, C. (2004) Profiling substrate fluxes in the isolated working mouse heart using 13C-labeled substrates: focusing on the origin and fate of pyruvate and citrate carbons. *Am. J. Physiol. Heart Circ. Physiol.* **286,** H1461–1470
27. O'Connell, T. D., Rodrigo, M. C., and Simpson, P. C. (2007) Isolation and culture of adult mouse cardiac myocytes. *Methods Mol. Biol.* **357,** 271–296
28. Luciani, D. S., Gwiazda, K. S., Yang, T. L., Kalynyak, T. B., Bychkivska, Y., Frey, M. H., Jeffrey, K. D., Sampaio, A. V., Underhill, T. M., and Johnson, J. D. (2009) Roles of IP3R and RyR Ca^{2+} channels in endoplasmic reticulum stress and β-cell death. *Diabetes* **58,** 422–432
29. Trollinger, D. R., Cascio, W. E., and Lemasters, J. J. (1997) Selective loading of Rhod 2 into mitochondria shows mitochondrial Ca^{2+} transients during the contractile cycle in adult rabbit cardiac myocytes. *Biochem. Biophys. Res. Commun.* **236,** 738–742
30. Ally, A., and Park, G. (1992) Rapid determination of creatine, phosphocreatine, purine bases and nucleotides (ATP, ADP, AMP, GTP, GDP) in heart biopsies by gradient ion-pair reversed-phase liquid chromatography. *J. Chromatogr.* **575,** 19–27
31. Buteau, J., Shlien, A., Foisy, S., and Accili, D. (2007) Metabolic diapause in pancreatic β-cells expressing a gain-of-function mutant of the forkhead protein Foxo1. *J. Biol. Chem.* **282,** 287–293
32. Planavila, A., Iglesias, R., Giralt, M., and Villarroya, F. (2011) Sirt1 acts in association with PPARα to protect the heart from hypertrophy, metabolic dysregulation, and inflammation. *Cardiovasc. Res.* **90,** 276–284
33. Nemoto, S., Fergusson, M. M., and Finkel, T. (2004) Nutrient availability regulates SIRT1 through a forkhead-dependent pathway. *Science* **306,** 2105–2108
34. Lionetti, V., Stanley, W. C., and Recchia, F. A. (2011) Modulating fatty acid oxidation in heart failure. *Cardiovasc Res.* **90,** 202–209
35. Son, N. H., Yu, S., Tuinei, J., Arai, K., Hamai, H., Homma, S., Shulman, G. I., Abel, E. D., and Goldberg, I. J. (2010) PPARγ-induced cardiolipotoxicity in mice is ameliorated by PPARα deficiency despite increases in fatty acid oxidation. *J. Clin. Invest.* **120,** 3443–3454
36. Schaeffer, P. J., Wende, A. R., Magee, C. J., Neilson, J. R., Leone, T. C., Chen, F., and Kelly, D. P. (2004) Calcineurin and calcium/calmodulin-dependent protein kinase activate distinct metabolic gene regulatory programs in cardiac muscle. *J. Biol. Chem.* **279,** 39593–39603
37. Haemmerle, G., Lass, A., Zimmermann, R., Gorkiewicz, G., Meyer, C., Rozman, J., Heldmaier, G., Maier, R., Theussl, C., Eder, S., Kratky, D., Wagner, E. F., Klingenspor, M., Hoefler, G., and Zechner, R. (2006) Defective lipolysis and altered energy metabolism in mice lacking adipose triglyceride lipase. *Science* **312,** 734–737
38. Regazzetti, C., Peraldi, P., Grémeaux, T., Najem-Lendom, R., Ben-Sahra, I., Cormont, M., Bost, F., Le Marchand-Brustel, Y., Tanti, J. F., and Giorgetti-Peraldi, S. (2009) Hypoxia decreases insulin signaling pathways in adi-

pocytes. *Diabetes* **58,** 95–103
39. Croquelois, A., Domenighetti, A. A., Nemir, M., Lepore, M., Rosenblatt-Velin, N., Radtke, F., and Pedrazzini, T. (2008) Control of the adaptive response of the heart to stress via the Notch1 receptor pathway. *J. Exp. Med.* **205,** 3173–3185
40. Rohini, A., Agrawal, N., Koyani, C. N., and Singh, R. (2010) Molecular targets and regulators of cardiac hypertrophy. *Pharmacol. Res.* **61,** 269–280
41. Huang, X., Li, X., and Guo, B. (2008) KLF6 induces apoptosis in prostate cancer cells through up-regulation of ATF3. *J. Biol. Chem.* **283,** 29795–29801
42. Igwe, E. I., Essler, S., Al-Furoukh, N., Dehne, N., and Brüne, B. (2009) Hypoxic transcription gene profiles under the modulation of nitric oxide in nuclear run on-microarray and proteomics. *BMC Genomics* **10,** 408
43. Okamoto, Y., Chaves, A., Chen, J., Kelley, R., Jones, K., Weed, H. G., Gardner, K. L., Gangi, L., Yamaguchi, M., Klomkleaw, W., Nakayama, T., Hamlin, R. L., Carnes, C., Altschuld, R., Bauer, J., and Hai, T. (2001) Transgenic mice with cardiac-specific expression of activating transcription factor 3, a stress-inducible gene, have conduction abnormalities and contractile dysfunction. *Am. J. Pathol.* **159,** 639–650
44. Koh, I. U., Lim, J. H., Joe, M. K., Kim, W. H., Jung, M. H., Yoon, J. B., and Song, J. (2010) AdipoR2 is transcriptionally regulated by ER stress-inducible ATF3 in HepG2 human hepatocyte cells. *Febs J.* **277,** 2304–2317
45. Fisch, S., Gray, S., Heymans, S., Haldar, S. M., Wang, B., Pfister, O., Cui, L., Kumar, A., Lin, Z., Sen-Banerjee, S., Das, H., Petersen, C. A., Mende, U., Burleigh, B. A., Zhu, Y., Pinto, Y. M., Pinto, Y., Liao, R., and Jain, M. K. (2007) Kruppel-like factor 15 is a regulator of cardiomyocyte hypertrophy. *Proc. Natl. Acad. Sci. U.S.A.* **104,** 7074–7079
46. Yamamoto, K., Sakaguchi, M., Medina, R. J., Niida, A., Sakaguchi, Y., Miyazaki, M., Kataoka, K., and Huh, N. H. (2010) Transcriptional regulation of a brown adipocyte-specific gene, UCP1, by KLF11 and KLF15. *Biochem. Biophys. Res. Commun.* **400,** 175–180
47. Takeshima, H., Komazaki, S., Hirose, K., Nishi, M., Noda, T., and Iino, M. (1998) Embryonic lethality and abnormal cardiac myocytes in mice lacking ryanodine receptor type 2. *EMBO J.* **17,** 3309–3316
48. Zou, Y., Liang, Y., Gong, H., Zhou, N., Ma, H., Guan, A., Sun, A., Wang, P., Niu, Y., Jiang, H., Takano, H., Toko, H., Yao, A., Takeshima, H., Akazawa, H., Shiojima, I., Wang, Y., Komuro, I., and Ge, J. (2011) Ryanodine receptor type 2 is required for the development of pressure overload-induced cardiac hypertrophy. *Hypertension* **58,** 1099–1110
49. Santiago, D. J., Curran, J. W., Bers, D. M., Lederer, W. J., Stern, M. D., Ríos, E., and Shannon, T. R. (2010) Ca sparks do not explain all ryanodine receptor-mediated SR Ca leak in mouse ventricular myocytes. *Biophys. J.* **98,** 2111–2120
50. Pacher, P., Thomas, A. P., and Hajnóczky, G. (2002) Ca^{2+} marks: miniature calcium signals in single mitochondria driven by ryanodine receptors. *Proc. Natl. Acad. Sci. U.S.A.* **99,** 2380–2385
51. Denton, R. M., and McCormack, J. G. (1985) Ca^{2+} transport by mammalian mitochondria and its role in hormone action. *Am. J. Physiol.* **249,** E543–554
52. Wan, B., LaNoue, K. F., Cheung, J. Y., and Scaduto, R. C., Jr. (1989) Regulation of citric acid cycle by calcium. *J. Biol. Chem.* **264,** 13430–13439
53. Ueno, M., Suzuki, J., Zenimaru, Y., Takahashi, S., Koizumi, T., Noriki, S., Yamaguchi, O., Otsu, K., Shen, W. J., Kraemer, F. B., and Miyamori, I. (2008) Cardiac overexpression of hormone-sensitive lipase inhibits myocardial steatosis and fibrosis in streptozotocin diabetic mice. *Am. J. Physiol. Endocrinol. Metab.* **294,** E1109–1118
54. Liao, R., Jain, M., Cui, L., D'Agostino, J., Aiello, F., Luptak, I., Ngoy, S., Mortensen, R. M., and Tian, R. (2002) Cardiac-specific overexpression of GLUT1 prevents the development of heart failure attributable to pressure overload in mice. *Circulation* **106,** 2125–2131
55. Cullingford, T. E., Butler, M. J., Marshall, A. K., Tham el, L., Sugden, P. H., and Clerk, A. (2008) Differential regulation of Kruppel-like factor family transcription factor expression in neonatal rat cardiac myocytes: effects of endothelin-1, oxidative stress and cytokines. *Biochim. Biophys. Acta* **1783,** 1229–1236
56. Rutter, G. A., Burnett, P., Rizzuto, R., Brini, M., Murgia, M., Pozzan, T., Tavare, J. M., and Denton, R. M. (1996) Subcellular imaging of intramitochondrial Ca^{2+} with recombinant targeted aequorin: Significance for the regulation of pyruvate dehydrogenase activity. *P. Natl. Acad. Sci. U.S.A.* **93,** 5489–5494
57. Arrington, D. D., Van Vleet, T. R., and Schnellmann, R. G. (2006) Calpain 10: a mitochondrial calpain and its role in calcium-induced mitochondrial dysfunction. *Am. J. Physiol. Cell Physiol.* **291,** C1159–1171
58. Lehnart, S. E., Mongillo, M., Bellinger, A., Lindegger, N., Chen, B. X., Hsueh, W., Reiken, S., Wronska, A., Drew, L. J., Ward, C. W., Lederer, W. J., Kass, R. S., Morley, G., and Marks, A. R. (2008) Leaky Ca^{2+} release channel/ryanodine receptor 2 causes seizures and sudden cardiac death in mice. *J. Clin. Invest.* **118,** 2230–2245
59. George, C. H., Jundi, H., Thomas, N. L., Fry, D. L., and Lai, F. A. (2007) Ryanodine receptors and ventricular arrhythmias: emerging trends in mutations, mechanisms and therapies. *J. Mol. Cell Cardiol.* **42,** 34–50
60. Yamaguchi, N., Chakraborty, A., Pasek, D. A., Molkentin, J. D., and Meissner, G. (2011) Dysfunctional ryanodine receptor and cardiac hypertrophy: role of signaling molecules. *Am. J. Physiol. Heart Circ. Physiol.* **300,** H2187–H2195